Current Science International
Volume: 13 | Issue: 03| July – Sept.| 2024

EISSN:2706-7920 ISSN: 2077-4435
DOI: 10.36632/csi/2024.13.3.37
Journal homepage: www.curresweb.com
Pages: 433-447

Evaluation of the Efficiency of the Chitosan Nanoparticles for Immobilization and Optimization of α-Amylase Produced by *Aspergillus oryzae* F-923

Nagwa I. Omar[1], Shimaa S. Hanafy[1], Amr A. El-Ella[2] and M. Fadel[3]

[1]Biochemistry Department, National Research Centre, National Research Centre, ElBuhouth Street, P.O. 12622, Giza, Egypt.
[2]Department of Measurements Photochemistry and Agriculture Applications. National Institute of Laser Enhanced Science' Cairo University 'Giza' Egypt.
[3]Microbial Chemistry Department, National Research Centre, National Research Centre, ElBuhouth Street, P.O. 12622, Giza, Egypt.

Received: 25 July 2024 **Accepted:** 10 Sept. 2024 **Published:** 25 Sept. 2024

ABSTRACT

In this study, a partially purified α-amylase enzyme, was successfully produced by *A. oryzae* F-923 and immobilized with chitosan nanoparticles (Cs/GA-NPs). Various concentrations of chitosan nanoparticles were used for immobilization of α amylase enzyme. The highest immobilization yield was for 3 mg/ml concentration with 79.23%. The immobilized amylase enzyme and chitosan nanoparticles (Cs/GA-NPs) are assessed for quality using a number of factors, including native electrophoretic patterns, dynamic light scattering, zeta potential, and UV spectrum. For both free and immobilized α-amylase, the optimum pH levels were 6.5 and 5.5, respectively. The optimum reaction temperature for the immobilized amylase was at 45ºC, but it was optimum at 40ºC for free one. The K_m values for the immobilized and free amylases were 3.5 and 1.7 mg/reaction mixture, respectively. The V_{max} for the immobilized and free amylases were 1.25 and 4.76 U/mg, respectively.

Keywords: Chitosan nanoparticles, Immobilization, α-amylase and *A. oryzae* F-923

1. Introduction

α-Amylases enzymes (4-α-D-glucan glucanohydrolase, EC 3.2.1.1) catalyze the hydrolysis of internal α-1,4-glycosidic linkages in starch that result in producing small carbohydrate molecules consisting of glucose units (Ryan *et al.,* 2006). Based on the cleavage location, they are divided into three types: α-amylase, β-amylase, and γ-amylase. While γ-amylase cleaves α-1,6-glycosidic links, β-amylase hydrolyzes the second α-1,4-glycosidic bond, resulting in the cleavage of two glucose units. α-amylase cleaves at random positions throughout the starch chain (Das *et al.,* 2011 and Pandey *et al.,* 2000). It has been observed that microbial, animal, and plant sources produce amylases, but the most efficient has reportedly been found to be microbial amylase production (Gupta *et al.,* 2003 and Halima and Archna, 2023). Microorganisms are being used for a variety of applications, such as heavy metal absorption, digestion, gene editing, the creation of novel anti-microbials, and the manufacturing of industrial enzymes, as opposed to chemical approaches that demand severe conditions like temperature and high pressure (Prasad, 2011 and Tarhriz *et al.,* 2014).

The starch industry is the major industry consuming alpha-amylase. Enzymes are more suitable for processing starch although acid was used for the digestion of starch, due to their mild reaction conditions and fewer secondary reactions (Tarhriz *et al.,* 2024). Low stability is one of the main problems that enzymes face when used in the industrial field. Therefore, enhancing the stability of enzymes is necessary for industrial use. Many benefits, including as facile separation of the enzyme from the reaction mixture, effective recovery, and reusability, may come from the immobilization procedure (Mahboubi *et al.,* 2017; Nguyen *et al.,* 2017 and Mulko *et al.,* 2019).

Corresponding Author: Nagwa I. Omar, Biochemistry Department, National Research Centre, ElBuhouth Street, P.O. 12622, Giza, Egypt.
E-mail: nagwam2012@gmail.com

Chitosan is an amino polysaccharide made up of residues of N-acetylglucosamine and β-1,4-linked glucosamine, derived from the N-deacetylation process of chitin (Mulko *et al.,* 2020 and Sreekumar *et al.,* 2018). Chitosan exhibits various biological activities, including anticancer, antimicrobial, antioxidant, immune-stimulating, wound-healing, and anti-inflammatory properties (Takahashi *et al.,* 2008, Xu *et al.,* 2009; Malinowska-Pańczyk *et al.,* 2015 and Davydova *et al.,* 2016). The advantages of chitosan nanoparticles include a larger surface area, enhanced stability, improved adsorption power, and enhanced delivery capability (Harahap, 2012). Chitosan nanoparticles (nanoparticles, nanomaterials) is more effective at breaking through and penetrating bacterial cell membranes because of its high surface area and ratio factor (Vellingiri *et al.,* 2013).

Numerous techniques, including emulsification cross-linking, ionic gelation, reverse micellization, spray-drying, and nanoprecipitation, can be used to create chitosan nanoparticles (CNPs) (Riva *et al.,* 2011; Zhao *et al.,* 2011 and Silva *et al.,* 2017). Furthermore, emulsion droplet coalescence, emulsion solvent diffusion, desolvation, and modified ionic gelation with radical polymerization have all been employed (Shi and Fan, 2002). Molecular weight (MW), degree of deacetylation (DDA), and chitosan concentration are factors that influence CNP production in the ionic gelation process. Ionic gelation is the most prevalent process utilized in CNP manufacturing due to its simplicity of formation, rapidity, low cost (Mohammed *et al.,* 2017), and lack of organic solvents (Agnihotri *et al.,* 2004).

The characterization of CNPs is a very important step in evaluating the particles properties. Particle size, surface charge, morphological and surface features, and encapsulation efficiency are among of the parameters that are frequently employed to characterize CNPs. These characteristics shed light on the CNPs' stability, physicochemical activity, and cell absorption (Truong *et al.,* 2015 and Zhao *et al.,* 2017). Techniques based on imaging and non-imaging can be used to assess particle size. The decision is based on the estimated population and size of the CNPs. Light scattering, either dynamic light scattering (DLS) or static light scattering (SLS), is the basis of the non-imaging approach. These techniques are sensitive, quick, accurate, and helpful for measuring a variety of particle sizes (Kaasalainen *et al.,* 2017). Zeta potential is defined as the electrokinetic potential in colloidal systems, i.e., the difference between a point in the bulk fluid distant from the interface and the electric potential in the interfacial double layer at the site of the sliding plane (Neves *et al.,* 2017). Thus, the goal of this research was to evaluate the quality of chitosan nanoparticles prepared by crosslinking chitosan with glutraldehyde for immobilization of α-Amylase Produced by Aspergillus oryzae F-923.

2. Materials and Methods

2.1. Materials

Sodium hydroxide (NaOH), glutaraldehyde ($C_5H_8O_2$), chitosan powder with an 85% degree of deacetylation and low molecular weight (100-300 kDa), and soluble starch were all obtained from Sigma-Aldrich in Germany.

2.2. Methods

2.2.1. Preparation of amylase from *Aspergillus oryzae* F-923

2.2.1.1. Microorganism tested

Aspergillus oryzae F-923 was kept on potato dextrose agar (PDA) slants and kept at 4°C. It was obtained from the Microbial Chemistry Lab at the National Research Centre in Cairo, Egypt. It was periodically subcultured.

2.2.1.2. Experiments

The experiments were carried out in Erlenmeyer flasks with a volume of 250 ml, each holding 5 g of wheat bran and autoclaved for 20 minutes at 121°C.

2.2.1.3. Preparation of solid state fermentation for α- amylase

The spores were crushed and placed in 10 milliliters of sterile citrate phosphate buffer (pH 5.5) with 0.1% Tween 80 to create the fungal spore suspension. The growth substrate in the flasks was aseptically inoculated with 1 milliliter of the spore solution.

2.2.1.4. Extraction of Enzymes

Each flask holding the fermented cultures received acetone extraction solvent after a 72-hour incubation period at 28°C. The solvent was added in a ratio of 1:20 (w/v) substrate to solvent, along with 0.1% Tween 80. Using a rotary shaker, the flasks were shaken for 30 minutes at 30°C at 200 rpm. To get a clear filtrate, the contents of the flasks were filtered through Whatman filter paper No. 3.

2.2.1.5. Partial purification

Fadel *et al.* (2020) report that butanol was used to precipitate the protein included in the culture extract. To recover the cells and remaining medium, the crude culture filtrate from the previously stated enzyme extract was centrifuged at 10,000 rpm under chilling conditions. The pellet was then recovered by cooling centrifugation at 12,000 rpm for 10 minutes after the supernatant was precipitated overnight with butanol at a ratio of 1:4 (v/v). The pellets were again suspended in a little volume of pH 5.5 0.1M phosphate buffer.

2.2.2. α- amylase activity assay

Alpha-amylase activity of the extract was measured using the DNS method (Miller, 1959). The reaction mixture containing 2% soluble starch, 0.2 M phosphate buffer (pH = 5.5), and fermented extract was taken and incubated at 37°C for 30 minutes, followed by the addition of 3,5-dinitrosalicylic acid (DNS). With the use of a UV-VIS spectrophotometer, color development at 575 nm was measured in order to estimate the amount of reducing sugar released during the experiment. One unit (U) of amylase activity is defined as the amount of enzyme that liberates micromoles of maltose per minute under standard assay conditions.

2.2.3. Protein concentration Estimation

The protein concentration was determined using the Lowry *et al.* (1951) method, with a standard being bovine serum albumin.

2.2.4. Synthesis of Chitosan/glutaraldehyde-nanopaticles (Cs/GA-NPs) nanocomposites

The powdered chitosan was dissolved in one percent acetic acid., and the mixed solution was then agitated at 800 rpm at ambient temperature for more than 24 hours until a pure, viscous yellow solution of chitosan was formed. In order to create chitosan/glutaraldehyde nanoparticles (Cs/GA-NPs), an alkaline solution containing 2% NaOH was added to a chitosan stock solution to raise its pH to 8.0. A 1% solution of glutaraldehyde was used as a stabilizing agent, and the mixture was continuously stirred. The chitosan/glutaraldehyde nanoparticles (Cs/GA-NPs) nanocomposite was formed, resulting in a pale yellow color. Stable amine linkages were created through the crosslinking formation between the amine groups of the chitosan polymer and glutaraldehyde.

2.2.5. Immobilization of amylase onto Chitosan NPS

On 3 ml of chitosan nanoparticles, the alpha-amylase enzyme (0.1 ml solution in 0.2 M phosphate buffer, pH 5.5) was immobilized. Subsequently, the mixture was mixed and allowed to stir at room temperature for an hour (Zahraa *et al.,* 2022).

2.2.6. Ultraviolet absorption spectrum (UV)

The absorbance behavior of the chitosan nanoparticles and immobilized amylase was studied at 200-500 nm using the CECIL Instruments CE595 UV spectrophotometer (Inoue *et al.,* 1966).

2.2.7. Dynamic light scattering

Using Particle Sizing Systems, Inc., Santa Barbara, Calif., USA, the average hydrodynamic size of the produced chitosan-NPs was measured at room temperature and with a 90° detection angle. The samples were diluted with double-distilled water prior to analysis, and the run time was 49 seconds (Murdock *et al.,* 2008).

2.2.8. Zeta potential

The zeta potential of the dispersion was determined by Particle Sizing Systems, Inc., Santa Barbara, California, USA, at room temperature with a scattering angle of 13.8° and a run time of 2 minutes and 45 seconds. An electric field is applied across a dispersion to determine its zeta potential (Butsele *et al.,* 2009). With a velocity proportional to the zeta potential, particles in the dispersion will move in the direction of the electrode with the opposite charge.

2.2.9. Electrophoretic α‑amylase pattern

Polyacrylamide gel electrophoresis (PAGE) was supplied by this assay using Rammesmayer and Praznik's method (Rammesmayer and Praznik, 1992). After the electrophoresis run, the native gel was separated, cleaned with Tris–HCl buffer (pH 7.1), and then incubated with a working buffer that contained 0.5 g of soluble starch, 110 mg $CaCl_2$, and 50 mL of Tris–HCl (pH 7.5) (6 g /1L). In order to observe the α-amylase types that were separated by electrophoresis, they were placed in a staining solution that contained 300 mg of potassium iodide and 130 mg of iodine, both diluted in 100 milliliters of distilled water. The native isoamylase pattern was assessed using the Quantity One software (version 4.6.2) to ascertain the band percent (B%), band quantity (Qty), and relative mobility (Rf) of the electrophoretically separated bands after taking a picture of the PAGE plate. The proportions of physiological difference (Diff%) and similarity index (SI%) were computed using Nei and Li's algorithm (Nei and Li, 1979).

2.2.10. Effects of different pH on the activity of enzymes

In order to record the pH profile under standard assay conditions, small aliquots of the produced enzymes (free and immobilized amylases) were evaluated with two buffering agents, 0.2 M acetate (pH 4-5.8) and 0.2 M phosphate (pH 6.0-9.0).

2.2.11. Effect of different temperatures on enzyme activities

The activities of the produced enzymes (free and immobilized amylases) were evaluated at various incubation temperatures ranging from 30-70°C.

2.2.12. Effect of the reaction time on enzyme activities

Under standard assay conditions, the produced enzymes (free and immobilized amylases) were incubated with the substrate for varying durations up to 150 minutes in order to record the time profile.

2.2.13. Effect of different substrate concentrations on enzyme activities

The effect of different substrate concentrations was calculated by incubating various substrate concentrations ranging from 2 to 16 mg per reaction mixture for the free and immobilized amylase enzyme.

2.2.14. Determination of Michaelis' constant (K_m) and maximum velocity (V_{max})

Using the Lineweaver and Burk technique (Lineweaver and Burk, 1934), the Km and Vmax values of the free and immobilized amylases toward soluble starch were calculated.

3. Results and Discussion

3.1. Preparation of amylase from *Aspergillus oryzae* F-923

The α-amylase enzyme was successfully produced by A. oryzae F-923, a local strain, produced on wheat bran under a solid-state fermentation system by optimizing the production conditions (Fadel *et al*, 2020). The most promising isolate for the production of the α-amylase enzyme was *Aspergillus oryzae* F-923 which grown on wheat bran. The physical parameters of pH, temperature, incubation time, and moisture content were optimized at 5.5, 28°C, 72 hours and 1:2 (w/v), respectively. When ammonium sulfate was added to wheat bran as a nitrogen source, enzyme production increased. The addition of 10% (w/w) soluble starch to wheat bran as a carbon source also increased the production of α-amylase. The DNS technique was used to measure the extract's alpha-amylase activity. Soluble starch was used as the substrate, and the enzyme activity was run under standard reaction conditions. The enzyme's specific activity was 10.9 IU/mg protein.

3.2. Preperation of chitosan nanoparticles by crosslinking method

The chitosan/glutaraldehyde-nanopaticles (Cs/GA-NPs) nanocomposite with concentration 10 mg/ml was formed, the pale yellow color obtained of Cs/GA-NPs. Stable amine linkages were created through the crosslinking of the chitosan polymer's amine groups with glutaraldehyde. Ultraviolet spectrum was used to characterize the nanocomposite. The nanocomposite UV spectrum with different concentrations (3, 5, 7, 10 mg/ml) were carried out. As showed in Fig. (1), the ultraviolet absorbency profile of four concentrations. The results showed two sharp peaks identified in the UV-visible spectrum at 213 and 231 nm of 10 mg/ml and two peaks at 214 and 229 nm of 7 mg/ml. However, UV spectrum results of 5mg/ml and 3mg/ml showed the highest point at 223 and 213 nm, respectively. From these results, it was observed that sharpness and count of peaks decrease with decreasing of the concentration of chitosan nanoparticles. The positively charged amino groups in the chitosan molecule and the negatively charged groups of the polyanion or crosslinker combine to produce the complex that makes up the chitosan nanoparticles (Al-Nemrawi *et al.,* 2018). When chitosan is dissolved in an aqueous acidic solution, the amino group will be protonated to form -NH3+. Adding chitosan's cationic charges dropwise to a polyanionic solution while stirring continuously results in the formation of spherical hydrogel particles called chitosan nanoparticles (Neves Borgheti-Cardoso *et al.,* 2017).

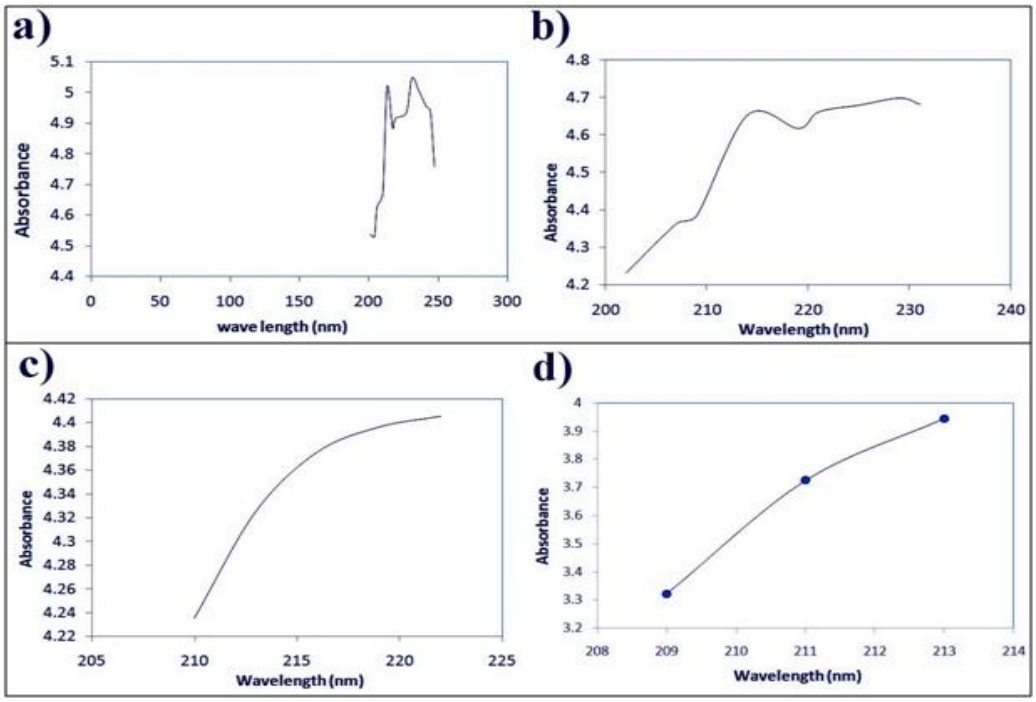

Fig. 1: Absorption spectrum of Chitosan/glutaraldehyde-nanopaticles (Cs/GA-NPs) with concentrations a) 10mg/ml, b) 7mg/ml, c) 5mg/ml and d) 3mg/ml

The size of particles scattered in a liquid can be determined using a method called dynamic light scattering. Due to its extreme sensitivity, big particles in a solution can also be measured using current systems. Fig. (2) showed the volumetric distribution of chitosan nanoparticles (CSNPs), which are produced when the chitosan polymer reacts with the glutaraldehyde crosslinker. The chitosan nanoparticles had an average diameter of 524.9 nm. In the present study, the UV absorbance and dynamic light scattering data indicated that the synthesized chitosan nanoparticles were successfully produced.

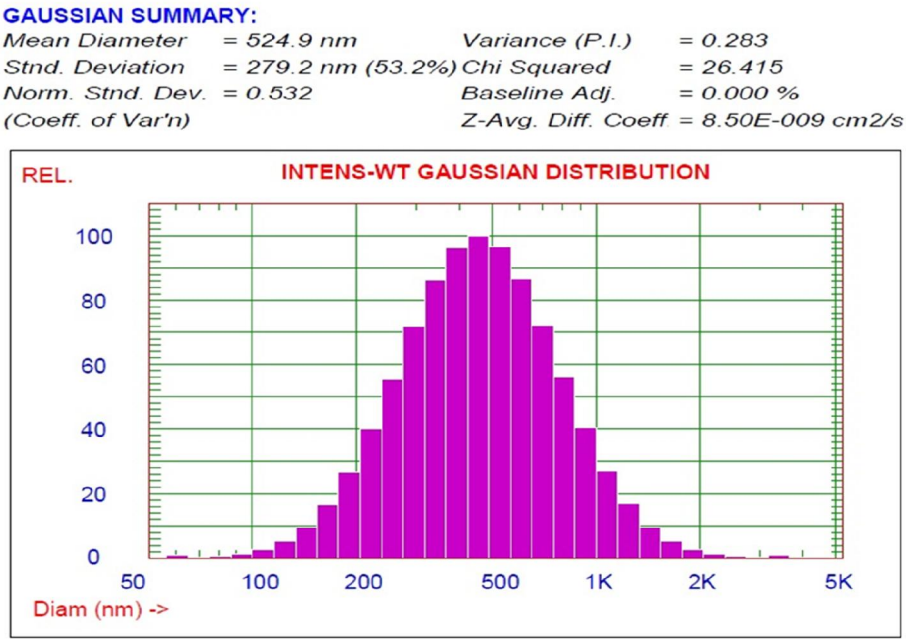

3.3. Immobilization of amylase by using different concentrations of chitosan nanoparticles

Various concentrations of chitosan nanoparticles (3, 5, 7 and 10 mg/ ml) were used for immobilization of α amylase enzyme. The immobilization yields of four concentrations were found to be 79.23, 42.3, 25.7 and 8.6 % for 3, 5, 7 and 10 mg/ml, respectively. Therefore, the highest immobilization yield was for 3 mg/ml concentration.

3.4. Characterization of chitosan nanoparticles, free amylase and immobilized amylase

3.4.1. The ultraviolet absorbency

The ultraviolet absorbency profiles of four immobilized amylases with different concentrations of chitosan nanoparticles showed in Fig. (3). The results showed three small peak identified at 214, 254 and 309 nm for 10 mg/ml concentration of chitosan nanoparticles and the sharpness of peak at 215 increased when the concentration of chitosan nanoparticles decreased for 7 and 5 mg/ml. However, UV spectrum results of 3mg/ml showed more peaks with more sharpness. These results illustrated the accumulation of amylase with the chitosan nanoparticles that lead to increase the absorbance and number of peaks. From these results, we could prove the immobilization process of amylase with chitosan nanoparticles was successfully done and 3 mg/ml of chitosan nanoparticles was the best one with the highest immobilization yield. These illustration is in corresponding with Guan *et al.* (2011).

3.4.2. Zeta potential

Zeta potential is the metric that determines the quality of nanoparticle yield. The electric charge that exists between colloidal particles is measured by a metric called zeta potential. The process of colloids merging from small to large is known as flocculation, and the higher the zeta potential value, the more it slows this process. The zeta potential measurements of the free enzyme, chitosan nanoparticles, and immobilized enzyme are presented in Fig. (4). Based on the results, the zeta potential value was 26.79 mV for chitosan nanoparticles, -27.88 for free enzyme and 25.43, -10.53, 30.60 and 8.06 for 3 mg/ml, 5mg/ml, 7mg/ml and 10mg/ml, respectively. According to the previous studies, it has been established that the nanoparticle formulation's zeta potential ranges from -30 to +30 mV (Coulmana *et al.,* 2009).

The stability of the nanoparticle dispersion system that was created is shown by the zeta potential value. Particles with a significant positive or negative zeta potential value generate a repulsive force between particles, according to Neves *et al.* (2017). In contrast, if the zeta potential value is low,

either positive or negative, it produces an attractive force between particles, resulting to the particles combining and becoming unstable.

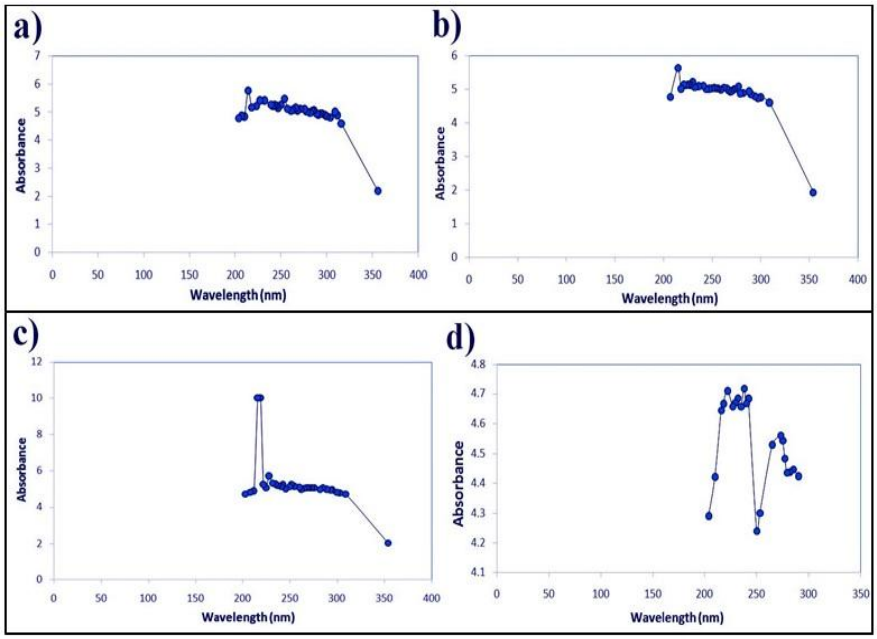

Fig 3: Absorption spectrum of immobilized amylase with Chitosan/glutaraldehyde-nanopaticles (Cs/GA-NPs) with concentrations **a)** 10mg/ml, **b)** 7mg/ml, **c)** 5mg/ml and **d)** 3mg/ml

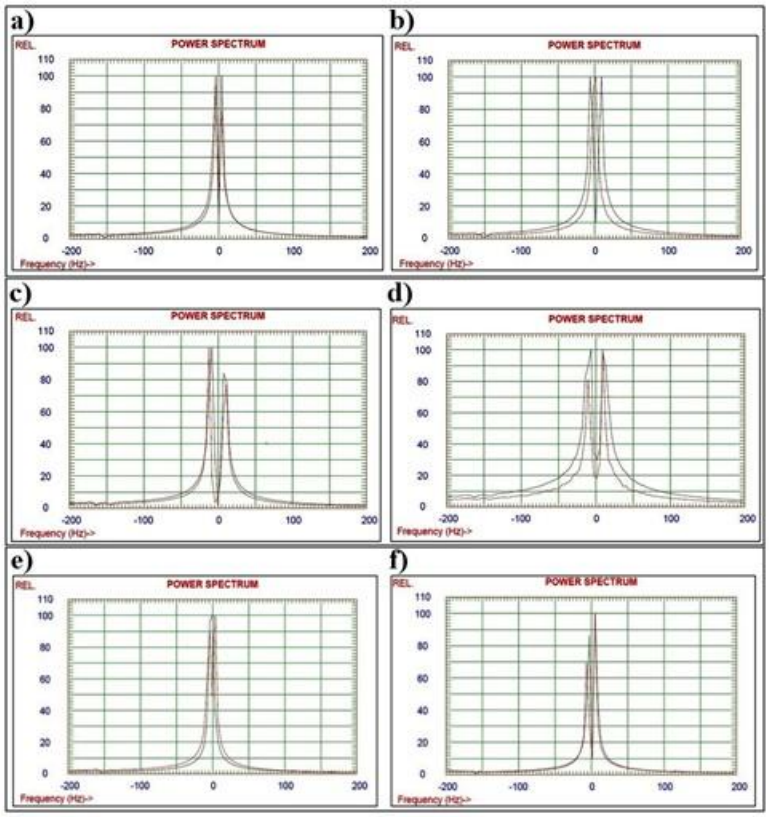

Fig. 4: Zeta potential of immobilized amylase with Chitosan/glutaraldehyde-nanopaticles (Cs/GA-NPs) with concentrations (**a)** 10mg/ml, **b)** 7mg/ml, **c)** 5mg/ml, **d)** 3 mg/ml), **e)** free α-amylase enzyme and **f)** chitosan nanoparticles

3.4.3. Native electrophoretic patterns.

Electrophoresis is the most common technique used for separating, recognizing, and quantifying different proteins and isoenzymes expressed in various tissues. It is frequently employed to examine the stoichiometry of a particular protein complex subunit (Aboulthana *et al.,* 2016). The electrophoretic patterns of chitosan nanoparticles, free, and immobilized amylases were demonstrated, and the primary results of native electrophoretic patterns are presented in Fig. (5).

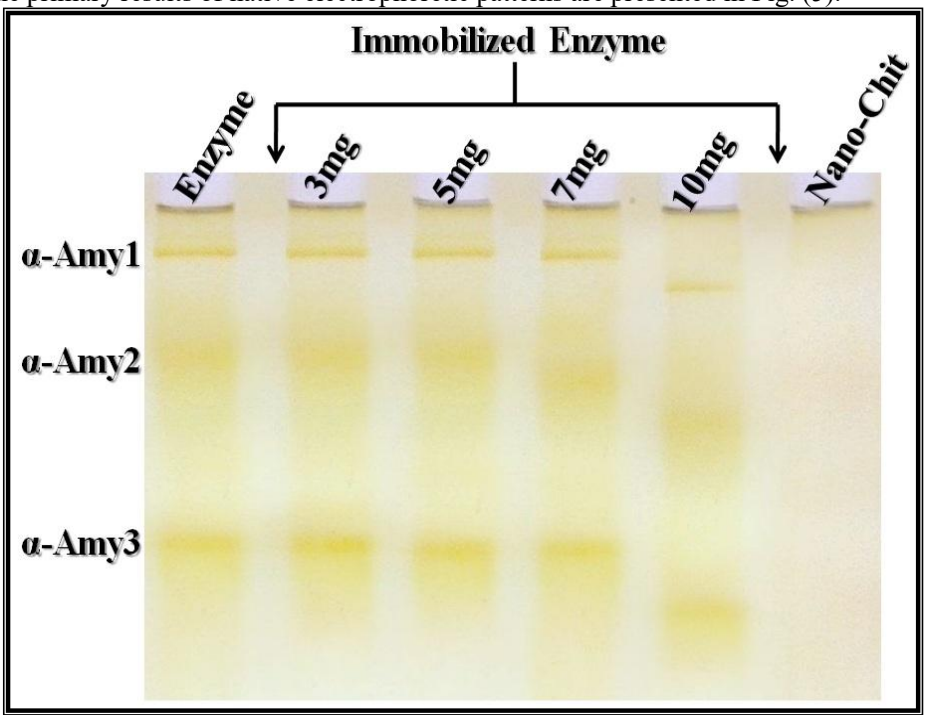

	Enzyme			Immobilized Enzyme												Nano-Chitosan		
				3 mg			5 mg			7 mg			10 mg					
	Rf.	Int.	B%	Rf.	Int.	B%	Rf.	Int.	B%	Rf.	Int.	B%	Rf.	Int.	B%	Rf.	Int.	B%
α-Amy1	0.07	245.88	26.47	0.07	288.33	50.87	0.07	324.20	43.76	0.07	288.28	51.20	-	-	-	-	-	-
	-	-	-	-	-	-	-	-	-	-	-	-	0.12	265.26	38.35	-	-	-
α-Amy1	0.22	141.23	15.21	0.22	170.04	30.00	0.22	168.16	23.00	0.23	94.49	16.78	-	-	-	-	-	-
	-	-	-	-	-	-	-	-	-	-	-	-	0.32	81.26	11.75	-	-	-
α-Amy1	0.50	541.69	58.32	0.50	108.42	19.13	0.51	248.53	33.55	0.51	180.27	32.02	-	-	-	-	-	-
	-	-	-	-	-	-	-	-	-	-	-	-	0.60	345.25	49.91	-	-	-
SI%	-			100.00			100.00			100.00			0.00			-		
Diff%	-			0.00			0.00			0.00			100.00			-		

Rf.: Relative Mobility, **Int.:** Band Intensity, **SI %:** Similarity Percent, **B %:** Band Percent **diff %:** Difference Percent.

Fig. 5: Native electrophoretic isoamylase pattern showing effect of chitosannanopartcles on the efficiency and physiological state of immobilized α-Amylase enzyme.

Electrophoresis can identify mutagenic differences at a qualitative assessment by distinguishing normal bands from the appearance of abnormal ones. The significance index (SI), which is inversely proportional to genetic variation and indicates qualitative changes, provides insights into on the physiological state of the tissue. A comparison of low SI values with the control group indicates

variations in the quantity and configuration of bands separated by electrophoresis. On the other hand, regular bands with their identity information are retained in quantitative modifications, and their amounts are altered.

As a result, electrophoretic α-amylase pattern in free and (3, 5, 7 mg/ml) immobilized appeared similar to the three standard isoamylases with (SI = 0.100%; Diff. = 00.00%), but in 10 mg/ml with (SI = 0. 00%; Diff. = 00.100%). Whether the electrophoretic pattern in chitosan nanoparticles with (SI = 0. 00%; Diff. = 00. 00%) because there are no bands appeared. In Fig. (6), the electrophoretic protein pattern demonstrates the effect of nano-chitosan on the amount of immobilized α-Amylase enzyme, as checked by SDS-PAGE. Furthermore, it presents the primary results from native electrophoretic patterns. From the above results, we choice 3 mg/ml for further study as a typical example of immobilization by covalent binding.

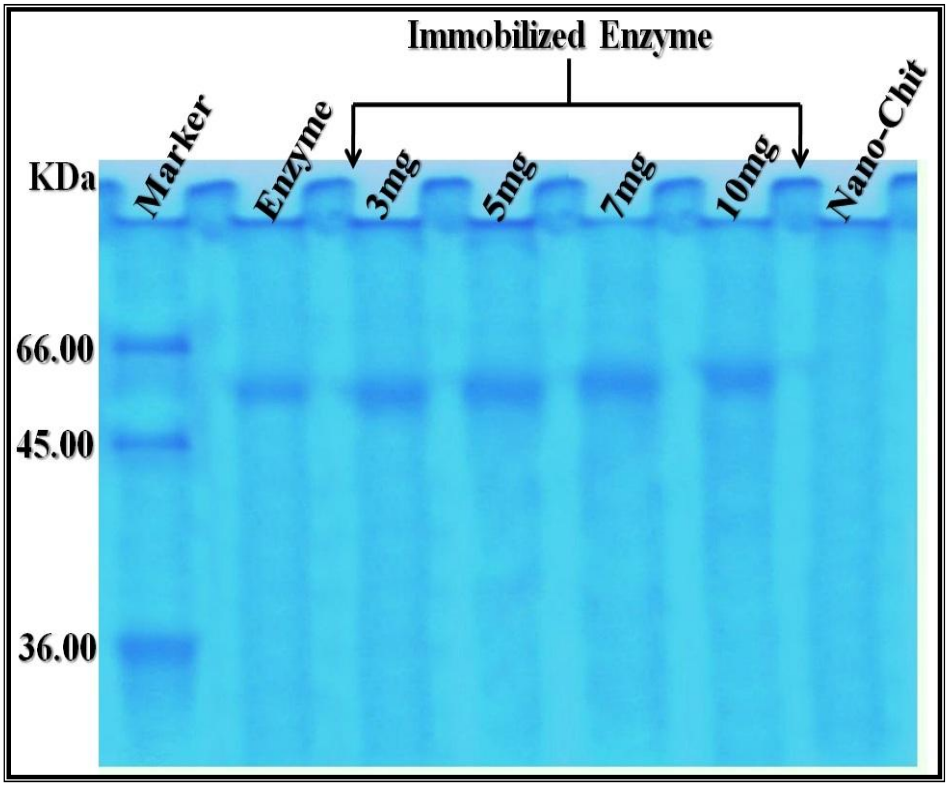

Mwts (KDa)	Enzyme			Immobilized Enzyme												Nano-Chitosan		
				3 mg			5 mg			7 mg			10 mg					
	Rf.	Mwt	Qty	Rf.	Mwt	Qty	Rf.	Mwt	Qty	Rf.	Mwt	Qty	Rf.	Mwt	Qty	Rf.	Mwt	Qty
66.00	-	-	-	-	-	-	-	-	-	-	-	-	-	-	-	-	-	-
-	0.32	55.57	12.35	0.33	54.71	16.75	0.32	55.57	20.80	0.31	57.34	20.46	0.30	58.24	17.35	-	-	-
45.00	-	-	-	-	-	-	-	-	-	-	-	-	-	-	-	-	-	-
36.00	-	-	-	-	-	-	-	-	-	-	-	-	-	-	-	-	-	-
Diff%	-			35.59			68.35			65.61			40.43			-		

Rf.: Relative Mobility, **Mwt:** Molecular Weight, **Qty:** Band Quantity, **Diff%:** Difference Percent in Band Quantity.

Fig. 6: Electrophoretic protein pattern showing effect of chitosannanoparticles on the quantity of the immobilized α-Amylase enzyme achieved by SDS PAGE.

3.5. Physicochemical properties of free and immobilized amylases.

3.5.1. Effect of different pH's on the specific activity of free and immobilized amylases.

One of the main factors that can change the activity of the enzymes in a reaction mixture is the pH. Because immobilization causes conformational changes in the enzymes, the optimum pH is typically shifted. Fig. (7) illustrates how pH affects the activity of free and immobilized α-amylase. For both free and immobilized α-amylase, the optimum pH levels were 6.5 and 5.5, respectively. These results is in agreement with Talekar *et al.* (2010).

Changes in pH result in the breaking of ionic bonds that bind the tertiary structure of the enzyme (Rosdee *et al.,* 2020). The concentration of bound metal cations decreases as the concentration of hydrogen ions rises because more hydrogen ions will compete with one another for any metal cationic binding sites on the enzyme. The concentration of hydroxyl ions rises in response to a drop in hydrogen ion concentration. This competition with enzyme ligands for divalent and trivalent cations results in the conversion of these cations to hydroxides. The enzyme begins to lose its functional structure, notably the shape of the active site, so that the substrate no longer fits into it and the enzyme becomes denatured (Chattopadhyay and Mazumdar, 2000).

3.5.2. Effect of different temperatures on specific activity of free and immobilized amylases.

The enzyme activity is also strongly dependent on temperature. The effect of various degrees of temperature (30, 40, 45, 50, 55, 60, 65, and 70°C) on free and immobilized amylase activities was demonstrated in Fig. (8). The optimum reaction temperature for immobilized amylase ranged from 40 to 55°C with an optimum at 45°C, while it ranged from 40 to 50°C with an optimum at 40°C for the free enzyme. The changes in the physical and chemical properties of the immobilized chitosanase lead to an increase in the optimum temperature.

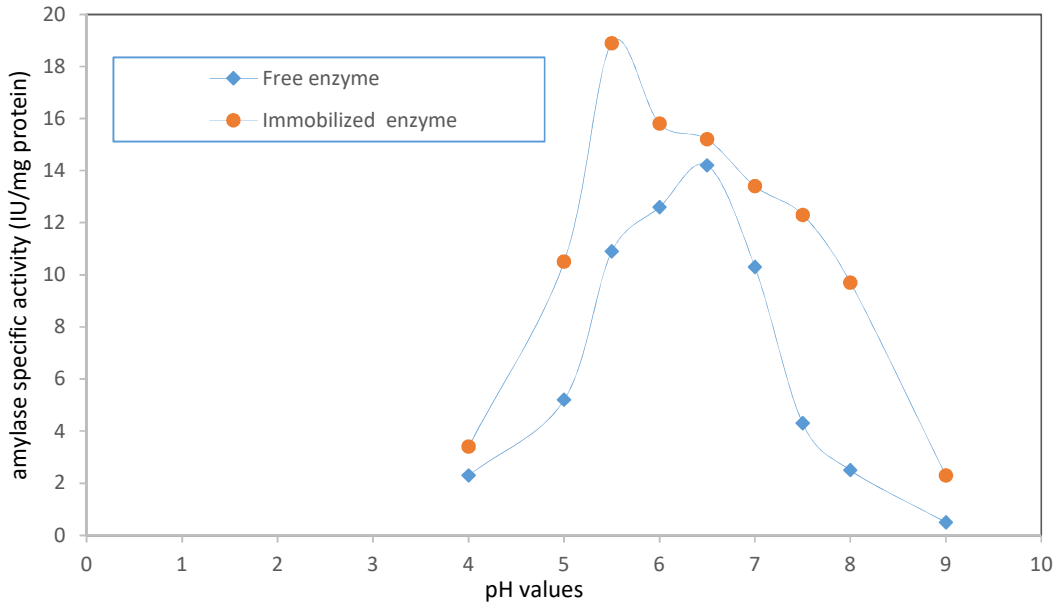

Fig. 7: Effect of different pH values on the specific activity of free and immobilized amylases.

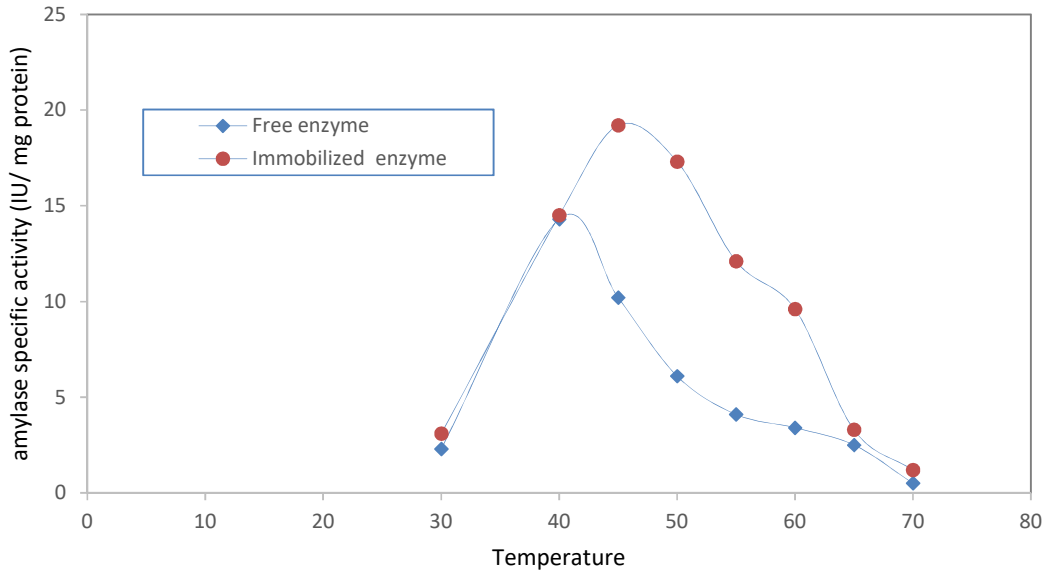

Fig. 8: Effect of different temperature on the specific activity of free and immobilized amylases.

3.5.3. Effect of the incubation time on free and immobilized amylases specific activities.

The specific activity of immobilized amylase was increased with increasing time of incubation during the first 2h as shown in Fig. (9). After 2h incubation time, no significant increase in activity was observed. Over time, all proteins suffer saturation and subsequently lose their catalytic activity. Reactions catalyzed by enzymes can be reversed (Robinson, 2015). At the beginning, the reaction only went forward because there was little or no product present. But as the reaction continued, there was a significant accumulation of product, and there was a significant rate of the backward reaction. The rate of product formation slowed down as the incubation time increased, and if the incubation time was long, then the measured activity of the enzyme would decrease. The amount of product that will be released increases as the incubation time of the enzyme with its substrate increases (Singh *et al.,* 2020).

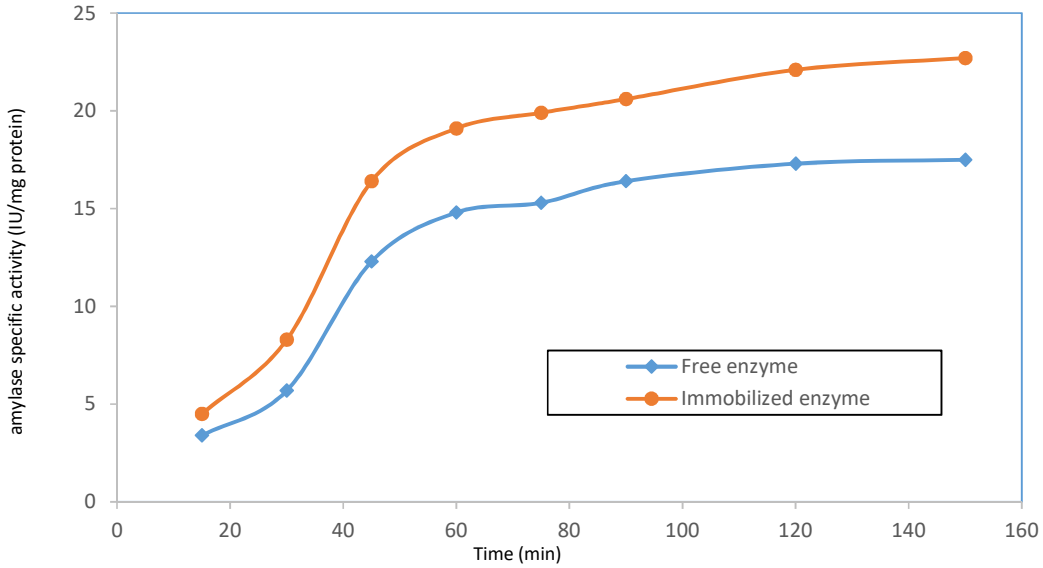

Fig. 9: Effect of different incubation times on the specific activity of free and immobilized amylase.

3.5.4. Effect of different substrate concentrations on free and immobilized amylases specific activities and the reaction kinetics.

Fig. (10) illustrate Linear relationships found between soluble starch and the specific activities of free and immobilized amylases up to 16 mg per reaction mixture for both free and immobilized amylases. The enzyme's catalytic site facilitates substrate binding, and the amount of substrate provided determines how quickly the reaction proceeds (Cleland, 1967). An enzyme with a high Km has a low affinity for its substrate, meaning that in order to reach V_{max}, the substrate concentration must be increased.

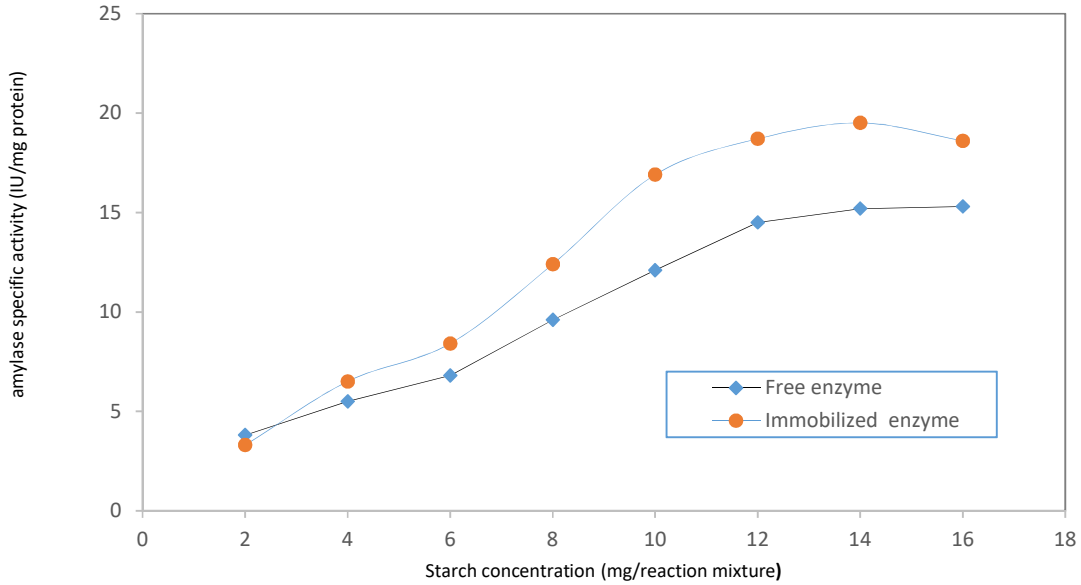

Fig. 10: Effect of different starch concentrations on the specific activity of free and immobilized amylase.

In Fig. (11, 12), the reaction kinetics of the free and the immobilized enzymes as estimated using Line-Weaver Burk (LB) plot under optimal conditions, indicate that the K_m values for the immobilized and free amylases were 3.5 and 1.7 mg/reaction mixture, respectively. The V_{max} for the immobilized and free amylases were 1.25 and 4.76 U/mg, respectively

These effects could be due to changes in enzyme configuration caused by immobilisation. This indicates that the conversion rate of substrate to product increased, but the affinity for substrate decreased. The results suggest that the immobilized enzyme has less specificity for the substrate. According to Singh *et al.* (2020) conformational changes in the structure of the enzyme may be responsible for a decrease in its kinetic characteristics upon immobilization.

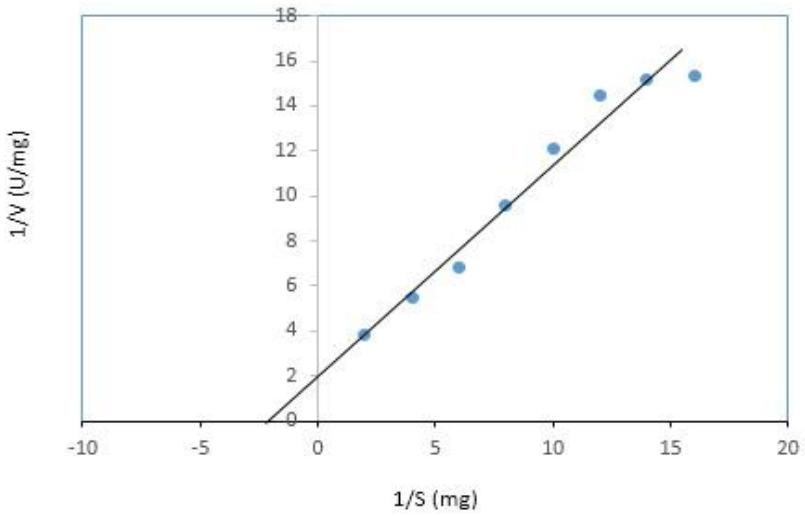

Fig. 11: Lineweaver-Burk plot for the free amylase enzyme using starch as substrate.

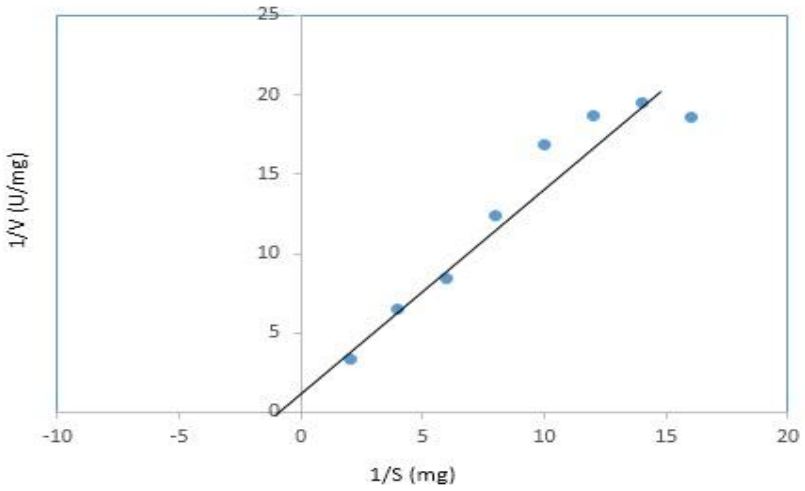

Fig. 12: Lineweaver-Burk plot for the immobilized amylase enzyme using starch as substrate.

4. Conclusion

The present study encompasses the kinetic behavior of α-amylase as free enzyme and immobilized enzyme with chitosan nanoparticles. The quality of the chitosan nanoparticles (Cs/GA-NPs) and immobilized amylase enzyme is assessed using a number of parameters, including zeta potential, dynamic light scattering, UV spectrum, and native electrophoretic patterns. Immobilized amylase showed high stability over a wide range of pH and temperature. Immobilized amylase showed increased enzymatic activity as compared to the free enzyme.

Acknowledgements

This work was accomplished practically in laboratories of the National Research Centre, Dokki, Giza, Egypt and provided by researchers of different scientific fields.

References

Aboulthana. W.M., M. Ismael and H.S. Farghaly, 2016. Int. J. Curr. Pharm. Res. 7: 347–359.
Agnihotri, S.A., N.N. Mallikarjuna and T.M. Aminabhavi, 2004. J. Control Release. 24: 5–28 .
Al-Nemrawi, N.K., S.S.M. Alsharif and R.H. Dave, 2018. Int. J. Appl. Pharm. 10: 60–65.

Butsele, K.V., P. Sibreta, C.A. Fustin, J.F. Gohyb, C. Passirani, and J.P. Benoitc, 2009. Synthesis and pH-dependent micellization of diblock copolymer mixtures. J. Colloid. Interf. Sci., 329: 235- 243.

Chattopadhyay, K., and S. Mazumdar, 2000. Structural and conformational stability of horseradish peroxidase: effect of temperature and pH. Biochemistry. 39(1): 263-70.

Cleland, W., 1967. Enzyme kinetics. Annual Review of Biochemistry. 36(1):77-112.

Coulmana, S.A., A. Anstey, C. Gateleyb, A. Morrisseyc, C. McLoughlind, C. Allendera, and J.C. Birchall, 2009. Microneedle mediated delivery of nanoparticles into human skin. Int. J. Pharm., 366: 190–200.

Das, S., S. Singh, V. Sharma, and M.L. Soni, 2011. Biotechnological applications of industrially important amylase enzyme. Int J Pharma Bio Sci. 2(1):486-96.

Davydova, V.N., A.A. Kalitnik, P.A. Markov, A.V. Volod'ko. S.V. Popov and I.M. Ermak, 2016. Appl Biochem Microbiol. 52: 476–482.

Guan, J., P. Cheng, S. Huang, J. Wu, Z. Li, X. You, and H. Zhang, 2011. Optimized preparation of levofloxacin-loaded chitosan nanoparticles by ionotropic gelation. Physics Procedia, 22: 163-169.

Gupta, R., P. Gigras, H. Mohapatra, V.K. Goswami, and B. Chauhan, 2003. Microbial α- amylases: a biotechnological perspective. Process Biochem., 38 :1599–616.

Halima, R. and N. Archna, 2023. Kinetics of immobilized alpha amylase impregnated with silver nanoparticles in Egg membrane for enhanced starch hydrolysis. Egypt. J. Chem., 66(2):1 – 12.

Harahap, Y., 2012. Preparation and characterization of chitosan nanoparticles with various acids. [Hon. Thesis]. Universitas Indonesia, Depok. [Indonesia].

Inoue, H., F. Suzuki, K.A. Fukunishi, K. Adachi, and Y. Takeda, 1966. Studies on ATP citrate lyase of rate liver. I. Purification and some properties. J. Biochem., 60: 543-553.

Kaasalainen, M., V. Aseyev, E. von Haartman, D.Ş. Karaman. E. Mäkilä, H. Tenhu, J. Rosenholm and J. Salonen, 2017. Nanoscale Res. Lett. 12: 74.

Lineweaver, H. and D. Burk, 1934. The determination of enzyme dissociation constant. J. Am. Chem. Soc., 56: 658-666.

Lowry, O.H., N.J. Rosebrough, A.L. Farr, and R.J. Randal, 1951. Protein measurement with the Folin phenol reagent. J. Biol. Chem. 193: 265-275.

Fadel, M., Sawsan AbdEl-Halim, Hayat Sharada, Y. Ahmed and Mayar Ammar, 2020. Production of Glucoamylase, α-amylase and Cellulase by Aspergillus oryzae F-923 Cultivated on Wheat Bran under Solid State Fermentation. J. Advances of Biology and Biotechnology (JABB), 23(4): 8-22.

Mahboubi, A., P. Ylitervo, W. Doyen, H. De Wever, B. Molenberghs, M.J. Taherzadeh, 2017. Continuous bioethanol fermentation from wheat straw hydrolysate with high suspended solid content using an immersed flat sheet membrane bioreactor. Bioresour Technol. 241:296-308.

Malinowska-Pańczyk, E., H. Staroszczyk, K. Gottfried, I. Kołodziejska and A. Wojtasz-Pająk . 2015. Polimery/Polymers. 60:735–741.

Miller, G.L., 1959. The use of dinitrosalicylic acid reagent for the determination of reducing sugars. Anal. Chem. 31: 426–428.

Mohammed, M.A., J.T.M. Syeda, K.M. Wasan and E.K. Wasan, 2017. Pharmaceutics. 9.

Mulko, L., J.Y. Pereyra, C.R. Rivarola, C.A. Barbero, and D.F. Acevedo, 2019. Improving the retention and reusability of alpha-amylase by immobilization in nanoporous polyacrylamide-graphene oxide nanocomposites. Int. J. Biol. Macromol. 122:1253-61.

Murdock, R.C., L. Braydich-Stolle, A.M. Schrand, *et al.,* 2008. Characterization of nanomaterial dispersion in solution prior to *in vitro* exposure using dynamic light scattering technique. Toxicol. Sci., 101: 239-53.

Nei, M. and W.S. Li, 1979. Mathematical model for studying genetic variation in terms of restriction endonuclease. Proc. Natl. Acad. Sci. 64. USA 76: 5269-5273.

Neves Borgheti-Cardoso, L., F. Vicentini, M. Cunha Filho and G. Gelfuso, 2017. In: Handbook of Composites from Renewable Materials. 285–308.

Nguyen, Q.A., E. Cho, L.T.P. Trinh, J.-S. Jeong, and H.-J. Bae, 2017. Development of an integrated process to produce d-mannose and bioethanol from coffee residue waste. Bioresour Technol. 244:1039-48.

Pandey, A., P. Nigam, C.R. Soccol, V.T. Soccol, D. Singh, and R. Mohan, 2000. Advances in microbial amylases. Biotechnol. Appl. Biochem., 31: 135–52.

Pramod, K.S., S. Renu, S. Manoj, D. Sibanada, M. Vellaichamy, P. Laccy and R. Bharti, 2024. Microbial production of α-amylase from agro-waste. Energy Nexus, 14 -100293

Prasad, N.K., 2011. Enzyme Technology: Pacemaker of Biotechnology. New Delhi: PHI Learning Pvt. Ltd.

Rammesmayer, G. and W. Praznik, 1992. Fast and sensitive simultaneous staining method of Q-enzyme, α-amylase, R-enzyme, phosphorylase and soluble starch synthase separated by starch: polyacrylamide gel electrophoresis. J. Chromatogr. 623(2):399–402.

Riva, R., H. Ragelle, A. des Rieux, N. Duhem, C. Jérôme and V. Préat, 2011. In: Jayakumar R, Prabaharan M and Muzzarelli RAA (eds) Chitosan for Biomaterials II. Springer Berlin Heidelberg, Berlin, Heidelberg, 19–44.

Robinson, P.K., 2015. Enzymes: principles and biotechnological applications. Essays in Biochemistry. 15;59.

Rosdee, N.A., N. Masngut, S.M. Shaarani, S. Jamek, and M.S. Sueb, 2020. Enzymatic hydrolysis of lignocellulosic biomass from pineapple leaves by using endo-1, 4-xylanase: Effect of pH, temperature, enzyme loading and reaction time. *In IOP Conference Series:* Materials Science and Engineering 736(2): 022095.

Ryan, S.M., G.F. Fitzgerald, and D. van Sinderen, 2006. Screening for and identification of starch-, amylopectin-, and pullulan-degrading activities in bifidobacterial strains. Appl Environ Microbiol., 72(8):5289-96.

Saeed, R.M., I. Dmour and M.O. Taha, 2020. Front Bioeng Biotechnol. 8: 1–21.

Shi, X.-Y. and X.-G. Fan, 2002. J. China Pharm Univ. 33:169–172.

Silva, M.M., R. Calado, J. Marto, A. Bettencourt, A.J. Almeida and L.M.D. Gonçalves, 2017. Mar Drugs. 15 : 370.

Singh. R.S., K. Chauhan and J.F. Kennedy, 2020. Fructose production from inulin using fungal inulinase immobilized on 3-aminopropyl-triethoxysilane. Biotechnology Reports 26: 41–52.

Sreekumar, S., and F.M. Goycoolea, 2018. Moerschbacher BM and Rivera-rodriguez GR. Sci. Rep. 1–11.

Takahashi, T., M. Imai, I. Suzuki and J. Sawai, 2008. Biochem. Eng. J. 40 : 485–491.

Talekar S., V. Ghodake, A. Kate, N. Samant, C. Kumar and S. Gadagkar, 2010. Preparation and characterization of crosslinked enzyme aggregates of Saccharomyces cerevisiae invertase. Aust. J. Basic Appl. Sci. 4:4760-4765.

Tarhriz, V., A. Hamidi, E. Rahimi, M. Eramabadi, P. Eramabadi, E. Yahaghi, *et al.,* 2014. Isolation and characterization of naphthalene-degradation bacteria from Qurugöl Lake located at Azerbaijan. Biosci Biotech Res Asia.11(2):715- 22.

Truong, N.P., M.R. Whittaker, C.W. Mak and T.P. Davis, 2015. Expert Opin Drug Deliv. 12 : 129–142.

Vellingiri, K., T. Ramachandran, and M. Senthilkumar, 2013. Eco-friendly application of nano chitosan in antimicrobial coatings in the textile industry. J Nanosci Nanotechnol 3 (4): 75-89.

Xu, Y., Z. Wen and Z. Xu, 2009. Anticancer Res. 29: 5103–5109.

Zahraa, S.A., A.T. Ali, N.A. Ahmed, and T.T. Noor, 2022. Immobilization of Urease onto Chitosan nanoparticles Enhanced the Enzyme Efficiency: Biophysical Studies and in Vitro Clinical Application on Nephropathy Diabetic Iraqi Patients. J. Nanotech.1-9.

Zhao, J., H. Lu, S. Wong, M. Lu, P Xiao and M.H. Stenzel, 2017. Polym. Chem. 8 : 3317–3326.

Zhao, L.M., L.E. Shi, Z.L. Zhang, J.M. Chen, D.D. Shi, J. Yang and Z.X. Tang, 2011. Brazilian J Chem Eng. 28: 353–362.